

Local Structure of Molten CdCl₂ Systems

Y. Okamoto^{a,b}, H. Shiwaku^b, T. Yaita^{a,b}, S. Suzuki^a, K. Minato^a, and H. Tanida^c

^a Department of Materials Science, Japan Atomic Energy Research Institute, Tokai-mura, Naka-gun, Ibaraki 319-1195, Japan

^b Synchrotron Radiation Research Center, Japan Atomic Energy Research Institute, Kouto, Mikazuki-cho, Sayo-gun, Hyogo-ken 6795143 Japan

^c Japan Synchrotron Radiation Research Institute, Kouto, Mikazuki-cho, Sayo-gun, Hyogo-ken 6795198 Japan

Reprint requests to Dr. Y. O.; Fax: +81-29-282-5922, E-mail: okamoto@molten.tokai.jaeri.go.jp

Z. Naturforsch. **59a**, 819–824 (2004); received June 25, 2004

The local structure of molten CdCl₂ was investigated by X-ray absorption fine structure (XAFS) and X-ray diffraction (XRD) analyses. The nearest Cd²⁺-Cl⁻ distance decreases from 2.61 Å in the room temperature solid state to 2.47–2.50 Å in the molten state. The coordination number decreases from 6 in the solid to 4 in the melt. The obtained structural parameters from the XAFS and the XRD analyses suggest that a tetrahedral coordination (CdCl₄)²⁻ is predominant in molten CdCl₂. The XAFS result of a molten 50% CdCl₂-KCl mixture shows that the 4-fold (CdCl₄)²⁻ structure holds also in the mixture.

Key words: Molten Salt; XAFS; X-ray Diffraction; Structure; Pyrochemistry.

1. Introduction

Pyro-electrochemistry [1], using molten salts, may become a reprocessing technology of spent nuclear fuels. For example, actinide metals are recovered with a cadmium cathode from the spent fuel [2]. Cadmium chloride is used for the recovery of ¹⁵N₂ gas, which is a component of nitride fuel [3]. Cadmium is also used for preparing transuranium chloride from metal [4]. Knowledge of the structure and physical properties of cadmium and its compounds is therefore very important for the development of pyrochemical processes of spent nuclear fuels.

Takagi et al. [5] studied the structure of molten CdCl₂ by using X-ray diffraction (XRD) and Raman scattering methods. They concluded that the local structure of molten CdCl₂ is tetrahedral (CdCl₄)²⁻. We have studied the structure and physical properties of some molten salts which are used in pyrochemical processes. For example, structural information on molten UCl₃, based on XRD [6] and X-ray absorption fine structure (XAFS) analyses was reported [7]. In the present study, the local structure of molten CdCl₂ and its mixtures with KCl was investigated by using high temperature XAFS. In addition, high temperature XRD measurements of molten CdCl₂ were performed to compare them with [5] and the present XAFS results.

2. Experimental

2.1. XAFS Measurement

The XAFS of molten CdCl₂ and CdCl₂-KCl was measured at the BL11XU beamline in the SPring-8 (Harima, Japan). The operating energy and the ring current were 8 GeV and 80–95 mA, respectively. Radiation monochromatized double diamond (111) crystals were used in the XAFS measurement. In this beamline, a gap of the insertion device (ID) is adjusted to obtain the strongest beam intensity for each energy. Thus, the strongest and continuous X-ray beam for a wide energetic range can be used in spite of the beamline with undulator. The XAFS spectrum for the Cd K-edge ($E_0 = 26.711$ keV) was obtained for each measurement.

Details of the high temperature XAFS measurements are described in [8]. The quartz cell, which consists of a upper storage tank for the solid sample, a quartz window for the XAFS measurement, and a bottom storage tank for the dropped melt was used. The sample of CdCl₂ (99.9% purity) was dried at 573 K under reduced pressure for 1 day to avoid moisture. When the upper tank was filled with the solid sample, it was sealed off under reduced pressure. The X-ray beam passes through the quartz window in trans-

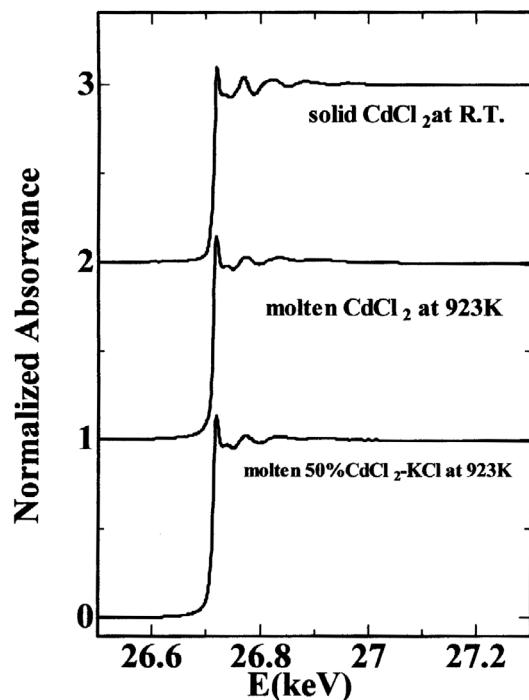


Fig. 1. Normalized X-ray absorption spectra of solid and molten CdCl₂ and molten 50% CdCl₂-KCl mixture.

mission XAFS measurements. No displacement of the baseline was detected in the empty cell. After heating over the melting point (841 K for CdCl₂), the cell was filled with the melt. The measurement was performed for 26.2 to 28.6 keV at 923 K.

The computer program code WinXAS ver.2.3., developed by Ressler [9], and the XAFS simulation code FEFF8 [10] was used in the XAFS data analysis. The phase shift and backscattering amplitude parameters, to be used in the curve fitting of the WinXAS, were simulated by using the FEFF8. The coordination number N_j , interionic distance r_j and Debye-Waller factor σ_j^2 were obtained from curve fitting in k -space. The cumulant expansion technique [11] was used to treat an anharmonic vibration effect. Thus, the following equation was used in the fitting procedure:

$$\chi(k) = \sum_j N_j S_j(k) F_j(k) \exp(-2\sigma_j^2 k^2) \exp(-r_j/\lambda) \cdot \exp\left(\frac{2}{3}C_4 j k^4\right) \sin\left(2kr_j + \phi_j(k) - \frac{4}{3}C_3 j k^3\right) / (kr_j^2),$$

where N_j = coordination number(CN) of the ion j around the central ion i , $S_j(k)$ = amplitude reduction factor, mainly due to many-body effects, $F_j(k)$ =

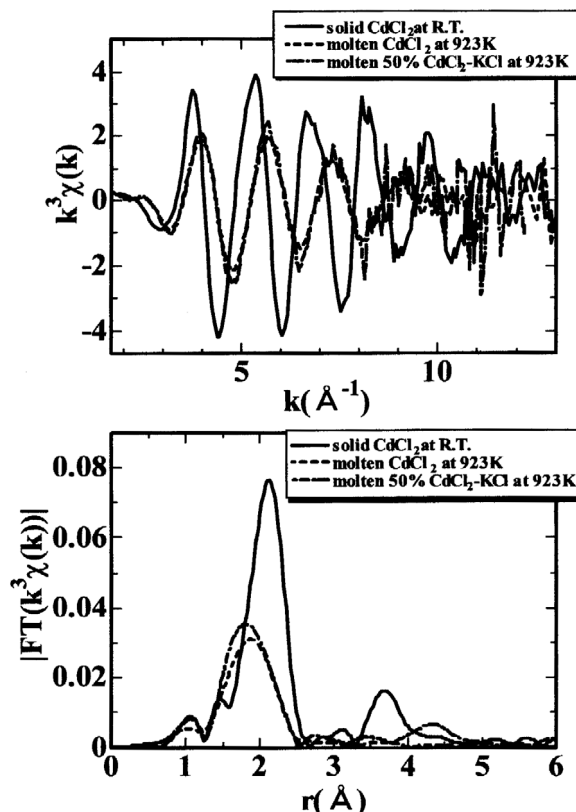


Fig. 2. XAFS functions $k^3\chi(k)$ and Fourier transform magnitudes $|\text{FT}(k^3\chi(k))|$ of solid and molten CdCl₂ and molten 50% CdCl₂-KCl mixture.

backscattering amplitude for each neighboring atom, σ_j = Debye-Waller factor corresponding to thermal vibration, λ = electron mean free path, $\phi_{ij}(k)$ = total phase shift experienced by the photoelectron, r_j = average distance of ion j from the central ion i , C_3, C_4 = 3rd and 4th cumulants.

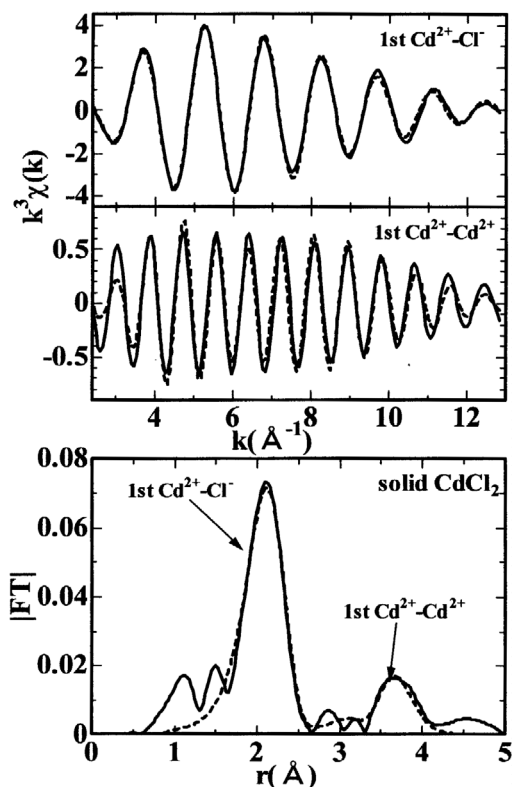
2.2. XRD Measurement

The XRD measurement was performed by using a Rigaku RINT2500TR diffractometer with 12.5 kW Mo-K α radiation (0.71069 Å). Details of the XRD measurement of molten salt systems were described in [12]. The CdCl₂ samples were sealed in a quartz cell (0.5 mm in thickness) under reduced pressure after drying at 573 K for 24 hours. The measurements were performed at 923 K. Fixed time scans were repeated several times from 5 to 55 degrees of the diffraction angle θ .

The reduced intensity function $Q_i(Q)$ was obtained by normalization of the raw intensity data to the elec-

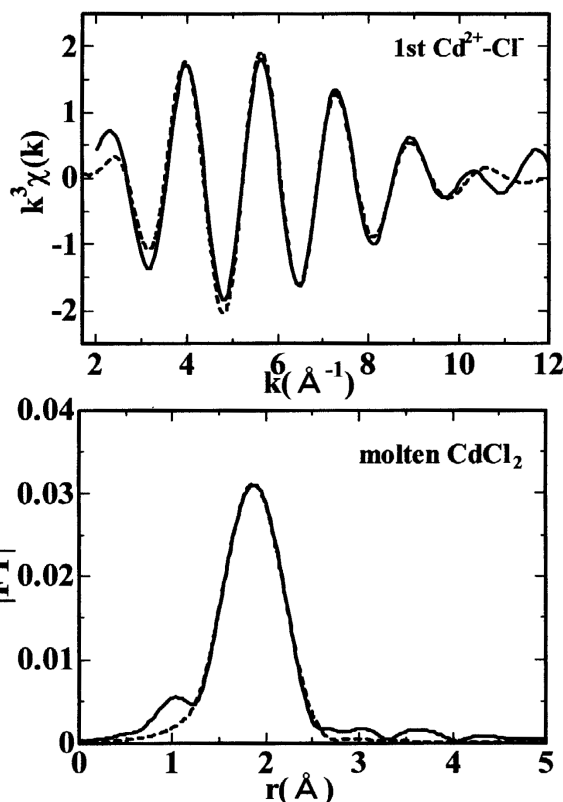
Table 1. Structural parameters of solid and molten CdCl₂ and molten 50%CdCl₂-KCl from Cd K-edge XAFS.

	$S_j(k)$	N_j	r_{ij} (Å)	σ_j^2 (Å ²)	C3 (10 ³ Å ³)	C4 (10 ⁴ Å ⁴)	Residual
solid CdCl ₂ :							
Cd ²⁺ -Cl ⁻	0.954	5.7	2.61	0.0105	—	—	8.7
Cd ²⁺ -Cd ²⁺		6.2	3.87	0.0173	—	—	
molten CdCl ₂ :							
Cd ²⁺ -Cl ⁻	0.819	3.8	2.47	0.0155	0.681	0.229	3.3
molten 50%CdCl ₂ -KCl:							
Cd ²⁺ -Cl ⁻	0.897	4.1	2.47	0.0147	1.072	0.938	8.1

Fig. 3. Curve fitting results of solid CdCl₂ at room temperature.

tron unit as described in [13]. The correlation function $G(r)$ was calculated from the $Q_i(Q)$ by fourier transformation. The interionic distance and coordination number of the 1st peak was estimated in the $G(r)$ function. In addition, the obtained $Q_i(Q)$ function was reproduced by the Debye scattering equation

$$Q_i(Q) = \sum_{i=1}^n \sum_j n_{ij} f_i(Q) f_j(Q) \exp(-b_{ij} Q^2) \cdot \sin(Qr_{ij})/r_{ij},$$

Fig. 4. Curve fitting results of molten CdCl₂ at 923 K.

where n_{ij} , r_{ij} and b_{ij} are the correlation number, interionic distance and temperature factor, respectively. The function $f_i(Q)$ is an atomic scattering factor of a lone atom i . The best structural model was obtained by using least squares fitting to the experimental $Q_i(Q)$ function.

3. Results and Discussions

3.1. XAFS

Figure 1 shows normalized X-ray absorbance spectra of solid CdCl₂ and molten CdCl₂ and 50%CdCl₂-KCl systems. Figure 2 shows XAFS functions $k^3\chi(k)$ and fourier transform functions $|FT|$ for solid CdCl₂ and molten CdCl₂ and 50%CdCl₂-KCl. In the XAFS function, a phase shift to higher k and decreasing amplitude were detected on melting. It corresponds to a shift to lower r and decreasing 1st peak intensity in R-space. The 1st peak in the $|FT|$ function is assigned to the nearest Cd²⁺-Cl⁻ interaction. The shift to lower r of the 1st peak shows that the 1st correlation distance decreases on melting. The decreasing amplitude

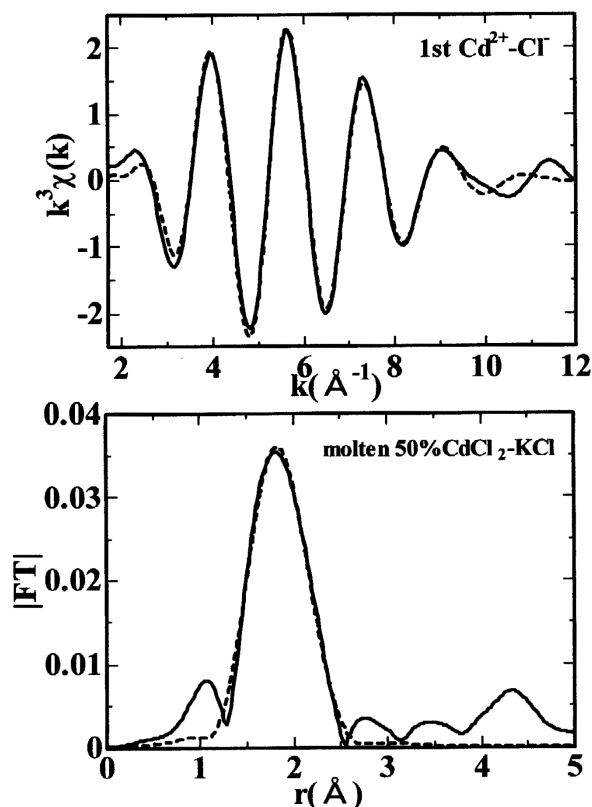


Fig. 5. Curve fitting results of molten 50%CdCl₂-KCl mixture at 923 K.

in $k^3\chi(k)$ and intensity of the 1st peak in the $|FT|$ function is assigned to a high temperature effect and/or decreasing coordination number. In solid state, the 2nd peak was observed around 3.6 Å in the $|FT|$ function. It is assigned to the 1st Cd²⁺-Cd²⁺ interaction. The 2nd peak was not observed around 3.6 Å in molten states. It implies that the correlation between the Cd²⁺ ions is small in the melts. The XAFS result of the mixture with KCl is close to that of the pure melt. It suggests that the local structure around the Cd²⁺ ion does not change by mixing with KCl.

Curve fitting results are shown in Figures 3–5. The structural parameters obtained by the fitting are listed in Table 1. In the fitting of solid CdCl₂ occur two kinds of interaction, Cd²⁺-Cl⁻ and Cd²⁺-Cd²⁺. The structural parameters of solid CdCl₂ are almost the same as those of CaF₂ with the density 4.08 g/cm³ [14]. By melting, the coordination number of the pair Cd²⁺-Cl⁻ decreases from 5.7 to 3.8. The interionic distance of the pair Cd²⁺-Cl⁻ decreases from 2.61 Å to 2.47 Å. The latter value is slightly larger than 2.42 Å, reported by

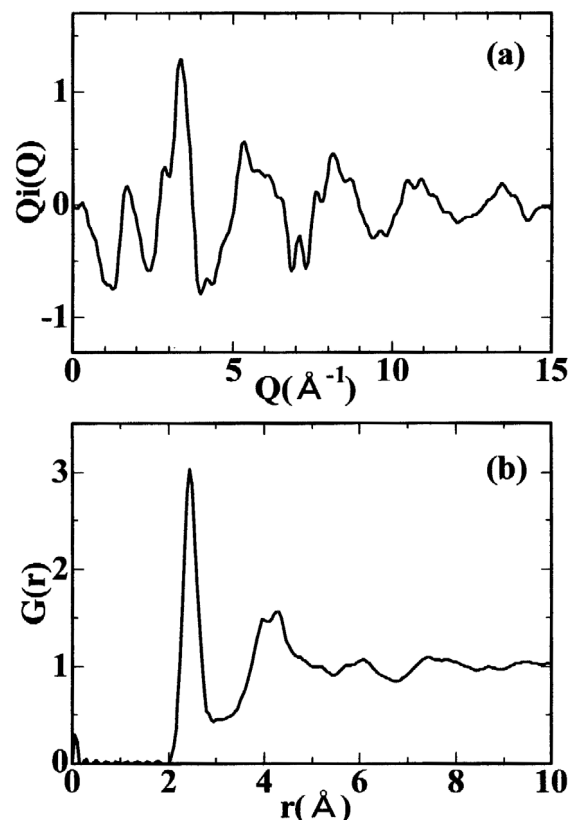


Fig. 6. X-ray reduced intensity function $Q_i(Q)$ and correlation function $G(r)$ of molten CdCl₂ at 923 K.

Takagi *et al.* [5]. The decrease of the Cd²⁺-Cl⁻ distance by 0.14 Å on melting is close to the difference between the ionic radii Cd(6-fold) = 0.95 Å and Cd(4-fold) = 0.78 Å [15]. The curve fitting results imply that the tetrahedral coordination (CdCl₄)²⁻ is predominant in the melt.

Structural parameters in the mixed melts are almost the same as those in pure CdCl₂ melt. Evidently the local structure does not change by mixing with alkali chloride. This is compatible with the Raman spectroscopic results on Cd²⁺ in molten LiCl-KCl-CdCl₂ by Børresen *et al.* [16].

3.2. XRD

The X-ray reduced intensity function $Q_i(Q)$ and the correlation function $G(r)$ of molten CdCl₂ are shown in Figs. 6(a) and (b), respectively. The $Q_i(Q)$ function shows a prepeak at $Q = 1.65 \text{ \AA}^{-1}$. This suggests that the melt has a rigid local structure and/or some network structure like zinc chloride melt [17] and rare

Table 2. The XRD Debye scattering parameters of molten CdCl₂.

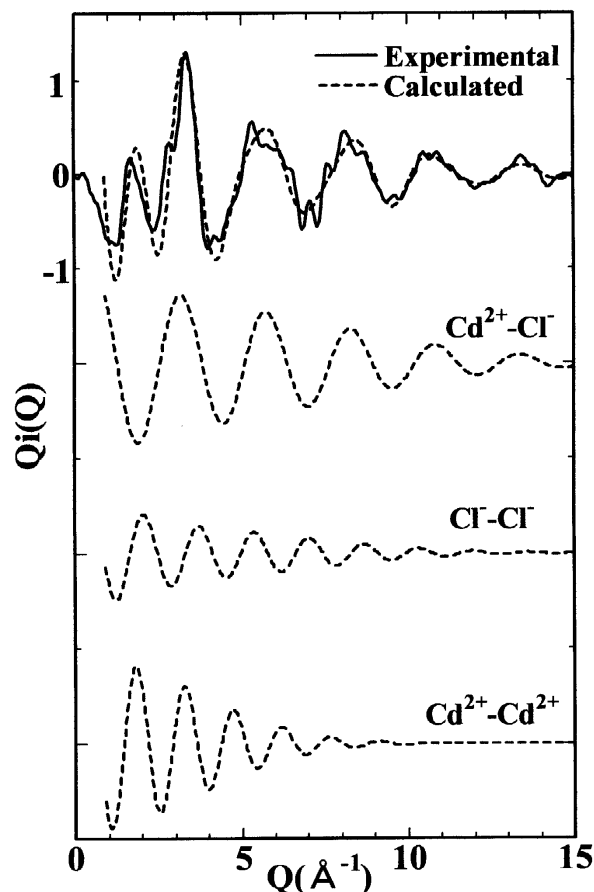
	$n_{ij}(N_{ij})$	r_{ij} (Å)	b_{ij} (Å ²)
Cd ²⁺ -Cl ⁻	4.1(8.2)	2.50	0.012
Cl ⁻ -Cl ⁻	10.3(20.6)	3.92	0.018
Cd ²⁺ -Cd ²⁺	5.1(5.1)	4.30	0.045

earth halide melts [18]. The sharp 1st peak at 2.50 Å in the $G(r)$ function is assigned to the nearest Cd²⁺-Cl⁻ correlation. This value is larger than 2.42 Å measured by Takagi *et al.* [5], and is slightly shorter than the sum of the ionic radii [15] $r[\text{Cd}(4\text{-fold}) + \text{Cl}] = 2.59$ Å. The coordination number, evaluated from the peak area with a cut-off distance $r_{\text{cut}} = 3.05$ Å is 4.1. These values are almost compatible with the XAFS result in the previous section. The 2nd peak at 3.9–4.4 Å is assigned to the 1st Cl⁻-Cl⁻ and Cd²⁺-Cd²⁺ correlations, though the peaks are not separated. These results imply that a 4-fold tetrahedral structure is most likely in the melt.

The reduced intensity function $Qi(Q)$ was reproduced by using the Debye scattering equation. In the fitting, a model expected from the $G(r)$ function was rigidly used to reduce computational errors and to avoid artificial fitting. At first, the parameters ($r(\text{Cd}^{2+}\text{-Cl}^-) = 2.50$ Å and coordination number = 4.1) of the nearest Cd²⁺-Cl⁻ correlation obtained directly from the $G(r)$ function were fixed in the fitting. Then a correlation with shorter distance in the 2nd peak of the $G(r)$ function was set to be the 1st Cl⁻-Cl⁻ pair, since it is naturally thought to be the interaction following to the nearest Cd²⁺-Cl⁻ pair. Finally, a distance of the Cd²⁺-Cd²⁺ pair was fixed to be 4.3 Å, since it is considered that the 2nd peak is mainly due to the Cd²⁺-Cd²⁺ correlation. The structural parameters as the result of least squares fitting were listed in Table 2. The calculated $Qi(Q)$ curves are shown in Fig. 7, together with partial contributions. The distance ratio $r(\text{Cl}^- \text{-Cl}^-)/r(\text{Cd}^{2+} \text{-Cl}^-) = 1.59$ is close to 1.633 in the right tetrahedron. It suggests that the local structure of CdCl₂ changes from 6-fold CaF₂-type to tetrahedral (CdCl₄)²⁻ structure on melting.

4. Conclusion

The local structure of molten CdCl₂ was investigated by using high temperature XAFS and XRD tech-

Fig. 7. Curve fitting results of molten CdCl₂ at 923 K.

niques. Both results show that the local structure of molten CdCl₂ changes from the CaF₂-type 6-fold to the 4-fold tetrahedral coordination (CdCl₄)²⁻ on melting. Although the result of molten CdCl₂ is close to the report by Takagi *et al.* [5], the Cd²⁺-Cl⁻ distance is significantly longer in the present work. The local structure around the Cd²⁺ ion does not change by mixing with KCl, since XAFS data of the mixture were close to those of the pure melt.

Acknowledgements

The authors gratefully acknowledge the interest and encouragement of Dr. Z. Yoshida and Dr. H. Ikezoe, and also thank Dr. J. Mizuki and Dr. T. Harami for support in the XAFS measurements at the SPring-8.

- [1] H. Takano, H. Akie, T. Osugi, and T. Ogawa, *Prog. Nucl. Energy* **30**, 373 (1998).
- [2] T. Kato, K. Uozumi, T. Inoue, O. Shirai, T. Iwai, and Y. Arai, *Proceedings of GLOBAL2003 Atoms for Prosperity: Updating Eisenhower's Global Vision for Nuclear Energy (CD-ROM)*, p. 1591 – 1595 (2003).
- [3] H. Hayashi, F. Kobayashi, and K. Minato, *J. Nucl. Sci. Tech. Suppl.* **3**, 624 (2002).
- [4] O. Shirai, T. Iwai, Y. Suzuki, Y. Sakamura, and H. Tanaka, *J. Alloys and Comp.* **271–273**, 685 (1998).
- [5] R. Takagi, N. Itoh, and T. Nakamura, *J. Chem. Soc., Faraday Trans. I* **85**, 493 (1989).
- [6] Y. Okamoto, F. Kobayashi, and T. Ogawa, *J. Alloys and Comp.* **271–273**, 355 (1998).
- [7] Y. Okamoto, M. Akabori, A. Itoh, and T. Ogawa, *J. Nucl. Sci. Tech. Suppl.* **3**, 638 (2002).
- [8] Y. Okamoto, M. Akabori, H. Motohashi, A. Itoh, and T. Ogawa, *Nucl. Instr. Meth. Phys. Res.* **A487**, 605 (2002).
- [9] T. Ressler, *J. Synchrotron Rad.* **5**, 118 (1998).
- [10] A. L. Ankudinov and J. J. Rehr, *Phys. Rev.* **B56**, R1712 (1997).
- [11] G. Bunker, *Nucl. Instrum. Methods Phys. Res.* **207**, 437 (1983).
- [12] Y. Okamoto, H. Hayashi, and T. Ogawa, *Japan J. Appl. Phys.* **38-1**, 156 (1999).
- [13] *Molten Salt Forum, Vol. 3, "X-ray Diffraction Analysis of Ionic Liquids"* ed. H. Ohno, K. Igarashi, N. Umesaki, and K. Furukawa, *Trans. Tech. Publications* 1994, Switzerland.
- [14] R. W. G. Wyckoff, *Crystal Structures, Vol. 1*, p. 270, John Wiley, New York 1963.
- [15] R. D. Shannon, *Acta Cryst.* **A32**, 751 (1976).
- [16] B. Børresen, G. A. Voyiatzis, and G. N. Papatheodorou, *Phys. Chem. Chem. Phys.* **1**, 3309 (1999).
- [17] M. C. C. Ribeiro, M. Wilson, and P. A. Madden, *J. Chem. Phys.* **109**, 9859 (1998).
- [18] F. Hutchinson, M. Wilson, and P. A. Madden, *J. Phys.: Condens. Matter* **12**, 10389 (2000).